



PbTe Quantum Dots and Engineering of the Energy Band Alignment in Photovoltaic Applications

Tuğba HACİFENDİOĞLU¹, Demet ASİL^{*1234}

¹Orta Doğu Teknik Üniversitesi, Kimya Bölümü, 06800, Ankara, Türkiye

²Orta Doğu Teknik Üniversitesi, Güneş Enerjisi Araştırma ve Uygulama Merkezi, 06800, Ankara, Türkiye

³Orta Doğu Teknik Üniversitesi, Mikro ve Nanoteknoloji, 06800, Ankara, Türkiye

⁴Orta Doğu Teknik Üniversitesi, Polimer Bilimi ve Teknolojisi, 06800, Ankara, Türkiye

*corresponding author e-mail: ademet@metu.edu.tr

(Received: 05.03.2021, Accepted: 06.09.2021, Published: 25.11.2021)

Abstract: Lead telluride (PbTe) quantum dots, despite being considered as one of the most promising candidates for future photovoltaics owing to their higher multiple exciton generation yields, have received limited attention in solar cell designs due their less explored surface chemistry and high air sensitivity. This study demonstrates the synthesis and characterization of highly crystalline PbTe QDs and their utilization in solution processed solar cells through band alignment engineering. Ultraviolet photoelectron spectroscopy showed that the conduction and valence band levels depend strongly on the type of surface ligand utilized for the ligand exchange process. Conduction and valence band levels of tetrabutylammonium iodide (TBAI) and 1,2-ethanedithiol (EDT) treated PbTe QDs with respect to vacuum were measured as -3.73 eV/-4.83 eV and -3.48 eV/-4.45 eV, respectively. The presence of a band offset between the conduction and valence band levels of TBAI and EDT treated layers allowed us to engineer the band alignment in the light absorbing layer. As a result, solar cells where TBAI and EDT ligand treated QDs were utilized in a bilayer cell architecture reached a photo conversion efficiency of 0.65%.

Key words: Lead telluride, PbTe quantum dots, Solar cells, TBAI, Band alignment

PbTe Kuantum Noktalar ve Fotovoltaik Uygulamalarda Bant Enerji Hizalamasının Yapılması

Öz: Kurşun tellür (PbTe) kuantum noktaları yüksek çoklu eksiton üretim verimine sahip olmaları nedeniyle fotovoltaik uygulama alanları için gelecek vaat eden adaylar olarak değerlendirilseler de görece daha az araştırılmış yüzey kimyaları ve atmosferik ortama olan hassasiyetleri sebebiyle güneş gözesi tasarımlarında sınırlı alaka görmektedirler. Bu çalışma, yüksek kristalli yapıya sahip PbTe kuantum noktalarının sentezini, karakterizasyonunu ve bant hizalama vasıtasıyla solüsyon bazlı güneş gözelerinde kullanımını konu almaktadır. Ultraviyole fotoelektron spektroskopisi çalışmaları, iletim ve değerlik bant seviyelerinin ligant değişimi işlemiyle kullanılan ligant türüne bağlı olduğunu göstermiştir. Tetrabutylamonyum iyodür (TBAI) ve 1,2-etanditiyol (EDT) ligantlarına tabi tutulmuş PbTe kuantum noktalarının vakuma karşı iletim ve değerlik bant seviyeleri sırasıyla -3,73 eV/-4,83 eV ve -3,48 eV/-4,45 eV olarak belirlenmiştir. TBAI ve EDT ligantlarıyla işlenmiş tabakaların arasında bulunan bant ofseti, güneşi soğuran tabakada bant hizalamasını gerçekleştirebilmemize olanak sağlamıştır. Sonuç olarak, TBAI ve EDT ligantları ile işlem görmüş kuantum noktalarının birlikte kullanıldığı çift katmanlı göze mimarisine sahip güneş gözeleri %0.65 foton değiştirme verimine ulaşmıştır.

Anahtar kelimeler: Kurşun tellür, PbTe kuantum nokta, Güneş gözesi, TBAI, Bant hizalama

1. Introduction

Solar energy harvesting technologies are essential to help reduce the reliance of industrialized nations on fossil fuels and to increase sustainable energy production for a decarbonized energy sector. Quantum dots (QDs), being excellent candidates for electronic applications, have been giving promising results and the efficiency of the laboratory scale solar cells has been reached up to 13.8% efficiency according to the recent reports [1]. Characteristic properties such as small band gap and large exciton Bohr radius of the lead chalcogenide QDs (PbX, X: S, Se, Te) make them excellent candidates for the visible and infrared photodetectors, photovoltaics, displays, and transistors [2–5].

Decreasing the mid gap state density in QDs has been shown to increase the efficiency of nanocrystal based solar cells in recent years [6–8]. Recent studies on PbSe QDs have shown that careful modification of the QD surface results in a notable improvement in the material quality and stability, and leads to an increase in the photovoltaic conversion efficiencies [7]. The last member of the lead chalcogenides family, PbTe QDs, although they are excellent candidates for electronic applications due to their higher multiple exciton generation yields [9], lag behind the other members of the lead based QDs due to less explored surface chemistry.

In general, three main methods are used to engineer QD surface for electronic applications; passivation on solid phase during the layer-by-layer process (L-B-L), injection of the passivation reagent during the growth phase and introduction of the passivating reagent to the already purified QDs in liquid phase. Generally used solid phase ligand exchange technique, L-B-L coating, has been one of the widely used methods to replace the original long chain, insulating hydrocarbon ligands, but also reported to have some detrimental effects due to harsh replacement of long insulating ligands with shorter ones on the solid phase. Halide passivation has been widely used to passivate PbS and PbSe QDs to improve the resistance of the QD surface against oxidative attacks and boost the photovoltaic efficiency [7]. Solution phase halide passivation attempts, on the other hand, yield QDs with lack of colloidal stability [10]. Recently introduced biphasic solution phase ligand exchange method has allowed oleyamine ligands to be exchanged with anionic ligands[11] or $\text{CH}_3\text{NH}_3\text{PbI}_3$ [12] in the solution phase. QDs that are ligand exchanged with this method are electrostatically stabilized and dispersible in polar solvents such as difluoropyridine (DFB) and butylamine (BA). However, for PbTe QDs, getting a uniform film with high crystallinity is not possible at all times due to the aggregation/precipitation of QDs. To overcome this problem and stabilize the dispersion, dimethylformamide (DMF) is required to be added to the BA or DFP solutions, which unintentionally decreases the concentration of QDs and the chances of getting thick films. Lack of reliable passivation protocols for PbTe QDs and a limited number of reports about the photovoltaic applications of PbTe QDs have motivated us to design a reliable PbTe QD passivation protocol with metal halides (RbI, CdI_2). This method stabilized PbTe QD thin films in ambient conditions and led to efficient photovoltaic devices based on passivated PbTe QDs for the first time [8]. Another halide containing surface ligand, tetrabutylammonium iodide (TBAI), has been successfully used for the ligand exchange process of PbS QDs and, through band alignment engineering, a bilayer cell architecture where TBAI treated PbS QDs were combined with 1,2-ethanedithiol (EDT) treated PbS QDs, produced solar cells with improved stability and photo conversion efficiency (PCE) [13].

Herein, we implement some recent advances in surface engineering methods developed for PbS and PbSe QDs to the PbTe QDs to improve ambient stability and long-term QD

solar cell stability. Halide containing TBAI ligand was utilized to improve air stability and solar cell parameters of PbTe QDs.

2. Material and Method

Trioctylphosphine (TOP, 90%, Sigma), lead (II) oxide (PbO, 99.999%, Sigma), diphenyl phosphine (DPP, 98%, Sigma), oleylamine (90%, Sigma), tetrabutylammonium iodide (TBAI, 99%, Sigma), oleic acid (OA, 90%, Sigma), 1,2-ethanedithiol (EDT, Sigma), titanium (IV) isopropoxide (TTIP, 99.999%, Sigma), 1-octadecene (ODE, 90%, Sigma) and tellurium powder (200 mesh, 99.999%, Alfa Aesar) were of the highest purity available and all the solvents were anhydrous.

Absorption spectra of the QDs prepared as dilute solutions in tetrachloroethylene (TCE) or as thin films spin coated on to the substrates were measured with a Shimadzu 3600 plus UV-Vis-NIR spectrometer. X-ray diffraction (XRD) measurements on thin films, prepared by spin coating on glass substrates, were performed with a high resolution Rigaku Ultima IV X-ray diffractometer with a Cu X-Ray source. A Jem Jeol 2100F 200kV high resolution transmission electron microscope (HRTEM) was used for imaging. Samples were prepared by drop casting QD solutions ($0.1-1 \text{ mg.ml}^{-1}$) on to 200 Mesh-carbon coated copper TEM grids in the glove box. QDs spin coated on Si/Cr (10 nm)/Au (150 nm) substrates were used for the X-ray and ultraviolet photoelectron spectroscopy (XPS/UPS) measurements. Monochromatic K X-ray (1,486.74 eV) and monochromatic HeI UV (21.2 eV) sources were used for the XPS and UPS measurements, respectively.

2.1 PbTe QD Synthesis and Passivation

PbTe QDs were synthesized according to literature reports [14,15]. The synthesis and purification processes were carried out in nitrogen filled Schlenk line and glove box in contrast to the generally used argon gas as an inert medium for highly sensitive PbTe QDs [9,16]. In a typical synthesis, 0.89 g PbO (4 mmol), 2.86 ml oleic acid (9 mmol), and 24.0 ml octadecene were combined in a three necked flask. The mixture was degassed under vacuum at $90^{\circ}\text{C}-100^{\circ}\text{C}$ for three hours. The reaction medium was taken under nitrogen flow and the temperature was raised to the injection temperature where 8.00 ml of 0.5 M TOP-Te with 4 μl DPP (DPP: Pb $1\mu\text{l}/1 \text{ mmol}$) solution was rapidly injected while vigorous stirring. TOP-Te stock solution was prepared by dissolving 6.38 g tellurium powder in 100 ml TOP and kept in a nitrogen filled glovebox for further use. The injection temperature was set as 150°C for $2.50 \pm 0.22 \text{ nm}$ PbTe QDs. After the injection, the dots were allowed to grow for 120 seconds while the temperature of the reaction medium was maintained at about 110°C with a temperature controller unit. The growth process was then rapidly terminated by injecting ice cold anhydrous hexane (10 ml) and placing the flask in an ice cold water bath. The crude solution was transferred to the glovebox for purification. Isopropyl alcohol (IPA)/acetonitrile (ACN) solvent mixture was added until maintaining a turbid solution and the solution was centrifuged for five minutes at 5000 rpm for further precipitation. After discarding the supernatant, the PbTe QDs were re-dispersed in hexane and precipitated by IPA/ACN or acetone two more times. PbTe QDs were kept in octane for the device fabrication or in tetrachloroethylene for the spectroscopic analysis.

2.2 Solar Cell Fabrication

Indium tin oxide (ITO) coated glass substrates were cleaned in acetone, IPA, and deionized water. TiO₂ electron transport layer was spin coated (at 5000 rpm) from a solution prepared by adding 1.25 ml of TTIP (0.60 mmol, 175 μ L) in ethanol to the hydrochloric acid diluted in 1.25 ml ethanol (2 M, 0.35 mmol, 17.5 μ L) [17]. The substrates were annealed at 450°C (30 minutes) in a muffle furnace and kept at room temperature in dark for at least 12 hours. Layer-by-layer (LBL) deposition technique was used for the preparation of PbTe QD active layer where the concentration of QD and TBAI solutions were set as 50 mg/ml in octane and 25 mg/ml in methanol, respectively. In a typical ligand exchange of OA-capped PbTe QDs with TBAI, the substrate was uniformly covered with PbTe QDs and spun after 5 s. Later, TBAI was introduced to the surface and spun after 30 s of wait. Residual ligands and un-exchanged PbTe QDs were removed by rinsing with methanol and octane, respectively. This cycle was repeated up to the desired thickness. Solar cells were encapsulated and legged after thermal evaporation of 80-100 nm thick Au electrode.

3. Results

A series of synthesis where the TOP-Te injection temperature was changed from 130°C to 160°C was performed to investigate the effect of growth temperature on size. Absorption and photoluminescence (PL) spectra of PbTe QDs, synthesized with the same Pb:OA:Te ratio at different growth temperatures, are presented in Figure 1a and Figure 1b. For the PL measurements, thin film (or solution) samples were excited at 980 nm with a laser diode and the PL emitted was detected by an InGaAs photodiode. The absorption peak points blue shift from 1200 nm to 1000 nm as the growth temperature decreases from 160°C to 130°C. Similarly, as shown in Figure 1b, the PL peak points red shift as the size increases. The relationship between the size and band gap is presented in Figure 1c. As the injection temperature increases, size of the QDs increases. Increase in size of the QD, from 2.5 nm to 5 nm, is accompanied by a decrease in band gap, from 1.4 to 0.8 eV, suggesting the presence of strong quantum confinement effects in PbTe QDs. TEM image of 5 nm PbTe QDs, prepared by drop casting of a dilute QD solution on to a 200 mesh-carbon coated copper grids, is presented in Figure 2d. The appearance of lattice fringes with a high resolution points out the high degree of purity and crystallinity of the PbTe QDs utilized in this study.

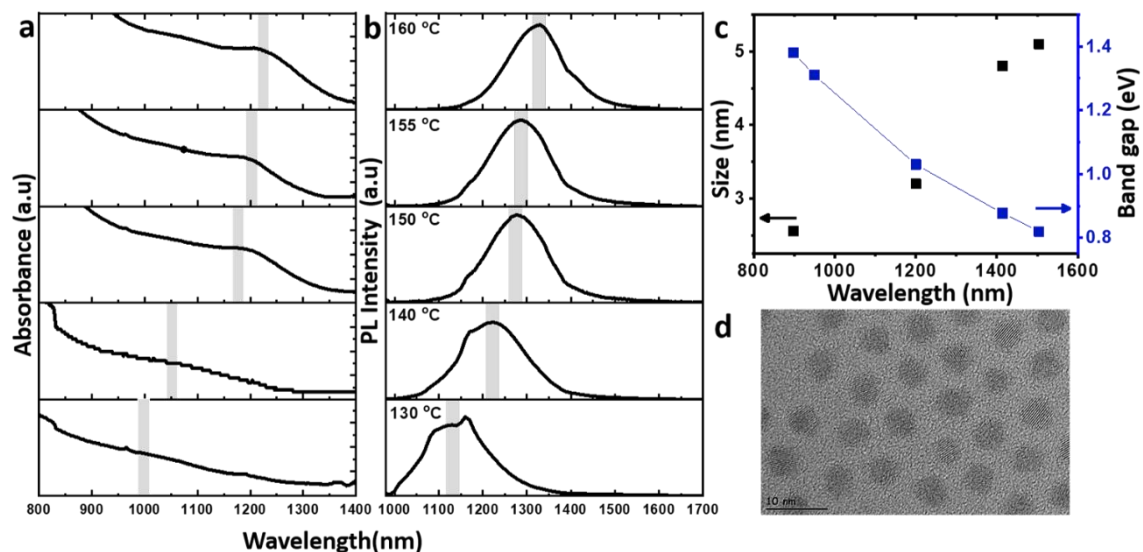


Figure 1. Change of absorbance (a) and photoluminescence (b) peak points with the injection/growth temperature. c) change of size with band gap. d) TEM image of PbTe QDs.

Native OA ligands were exchanged with TBAI or EDT to improve the conductivity of the QDs. The success of ligand exchange has been proved by Fourier transform infrared spectrometer (FTIR). FTIR spectra, shown in Figure 2c, indicate the partial removal of the oleate ligands for PbTe QD thin films. Strong C–H vibrations at 2918 cm^{-1} and 2849 cm^{-1} , and COO– vibrations at 1451 cm^{-1} and 1558 cm^{-1} , were eliminated as a result of the L-B-L ligand exchange treatment. As represented in Figure 2a and 2b, the excitonic peaks of the QDs were preserved due to EDT and TBAI treatments. The absorption peak points of the EDT and TBAI treated PbTe QDs were measured as 1364 nm and 1340 nm. Red shift of the absorption peak, compared to pristine OA capped QDs, can be attributed to the reduced interparticle distances between QDs which leads to enhanced coupling. Higher red shift of the excitonic peak ($\sim 24\text{ nm}$) for EDT might be attributed to the greater coupling of the PbTe QDs in the presence of EDT. Air stability of the thin film samples of PbTe QDs was assessed by measuring the blue shift of the absorption signal upon exposure to ambient conditions [8]. The change of the absorption peak points of the EDT and TBAI treated PbTe QD thin films when stored under atmospheric conditions for three days is represented in Figure 2a and 2b. As shown in Figure 2a, the excitonic peak disappears in three days. Therefore, EDT treatment yields PbTe QD thin films that are prone to oxidation. On the other hand, TBAI treated thin film preserves its excitonic peak upon exposure to ambient. This suggests successful surface passivation and enhanced endurance towards oxidative attacks when TBAI is utilized as a surface ligand.

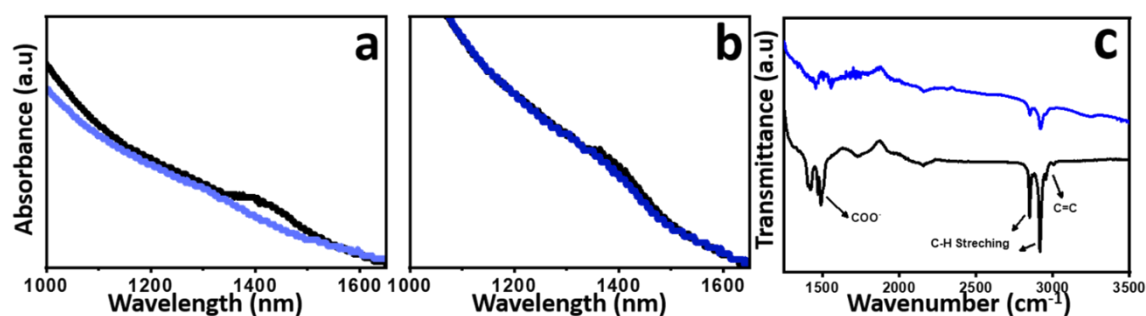


Figure 2. Thin film absorbance spectra of (a) EDT and b) TBAI treated PbTe QDs (black). Change of absorbance peak when thin films are exposed to ambient conditions for three days are presented with blue lines. c) FTIR spectra of as synthesized, OA capped (black) and ligand exchanged (blue) thin films.

PbTe QDs were characterized further with XRD to assess the crystallographic structure of the thin films. Thin film XRD patterns of the pristine, oleate stabilized PbTe QDs (JCPDS-ICDD card 38-1435) are represented in Figure 3b. The sharp peaks in the XRD profile indicate the high crystallinity of the PbTe QDs and confirm the crystalline phase purity of the PbTe, in accordance with the TEM image presented in Figure 1d. XRD patterns of pristine PbTe QDs surrounded by oleic acid stabilizing ligands show peaks at 23.60° , 27.65° , 39.70° and 47.80° corresponding to (111), (200), (220) and (311) diffractions. The diffraction peak at 27.65° corresponding to (200) is the most prominent peak, which can be assigned to the prominent growth orientation of PbTe nanostructures along the [200] direction. The distances between the adjacent lattice fringes shown in Figure 1d were measured as $3.2 \pm 0.1\text{ \AA}$, in line with the PbTe (200) d spacing of 3.23 \AA . XPS technique was utilized to characterize the surface atoms. Monochromatic K X-ray ($1,486.74\text{ eV}$) source was used for the XPS measurements.

Silicon substrates, on top of which 10 nm of Cr and 150 nm of Au were evaporated, were used for the measurements, and samples were prepared by spin coating QDs in the glove box. The spectrum was calibrated against the C1s peak (284.8 eV). Pb 4f and Te 3d5 spectra of pristine OA capped (solid line) and TBAI treated (dotted line) PbTe QDs are indicated in Figure 3a. The signals at 572.0 eV and 582.4 eV match with the binding energy of Pb–Te (Te-3d) [18]. Te-3d and Pb 4f peaks show a slight shift of ~0.6-0.8 eV to higher binding energies; 572.0 eV to 572.8 eV and 582.4 eV to 583.0 eV, respectively.

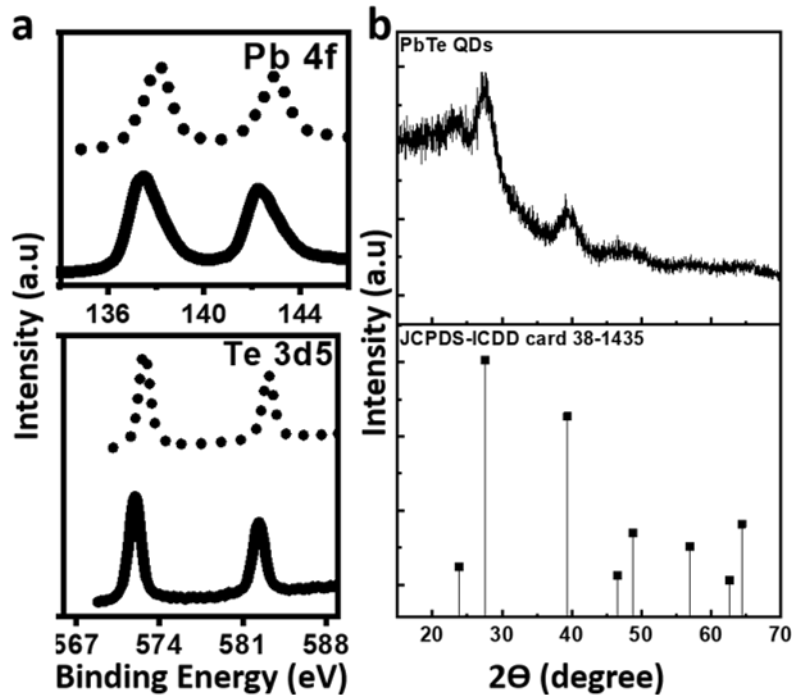


Figure 3 Pb 4f and Te 3d5 XPS spectra of pristine (solid line) and TBAI (dotted line) modified PbTe QDs. b) XRD pattern of PbTe QDs. XRD pattern of PbTe QDs with JCPDS-ICDD card 38-1435 is given as a reference.

We performed UPS measurements to investigate the Fermi level and the valence band maximum of PbTe QDs modified with TBAI and EDT. UPS spectra of PbTe QD thin films treated with TBAI and EDT on Si/Cr/Au substrates are displayed in Figure 4. The Fermi level of PbTe QDs treated with TBAI was determined by the difference between the incident photon energy (21.2 eV) and the binding energy of the high binding energy edge (secondary electron cut-off) [19]. The secondary electron cut-off, determined by the intersection of the linear part of the spectrum and the baseline, is 17.61 eV. The Fermi level was thus calculated as -3.59 eV ($\Phi = 21.2 - 17.6 = 3.59$ eV) with respect to vacuum. In order to determine the valence band maximum (E_V), the intersection of the linear portion of the spectra at low binding energy region with the baseline, corresponding to the difference between Fermi level and E_V , was determined. The difference between Fermi level and E_V was measured as 1.24 eV, corresponding to E_V of -4.83 eV ($E_V = -3.59 - 1.24$). To determine the conduction band minimum (E_C), the optical bandgap (E_g), determined from the absorption peak point, was added to E_V . The conduction band minimum of TBAI treated PbTe QD was calculated as -3.73 eV with respect to vacuum. The Fermi level for the EDT treated PbTe QDs was measured as -3.38 eV ($21.2 - 17.82$) with respect to vacuum. On the other hand, the difference between Fermi level and E_V was determined as 1.06 eV, which corresponds to an E_V of -4.45 eV with respect to vacuum.

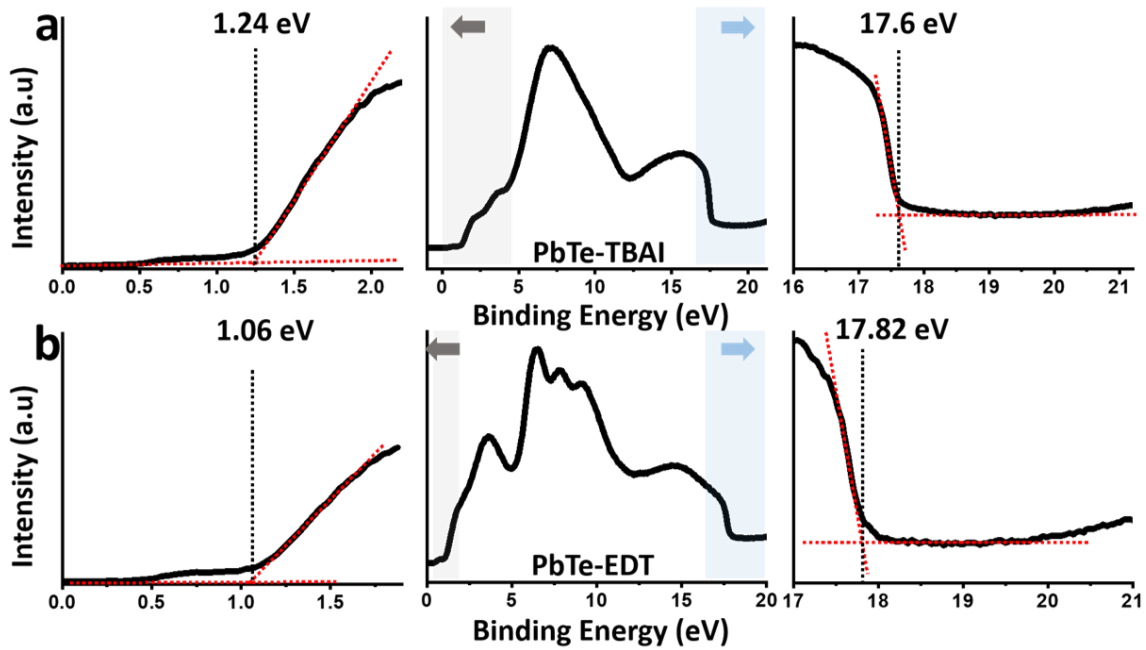


Figure 4 UPS spectra of a) TBAI and b) EDT treated PbTe QDs.

Energy landscape in TBAI and EDT treated PbTe QDs with respect to vacuum is shown in Figure 5c. According to the band levels estimated from UPS measurements, a band offset of about 0.25 eV exists between the conduction bands of TBAI and EDT treated layers. The presence of a band offset in the order of 0.25 eV suggest an efficient inhibition of electron back injection from PbTe-TBAI to PbTe-EDT. Furthermore, 0.38 eV band offset between their valence bands facilitates the hole transport from PbTe-TBAI to PbTe-EDT layers.

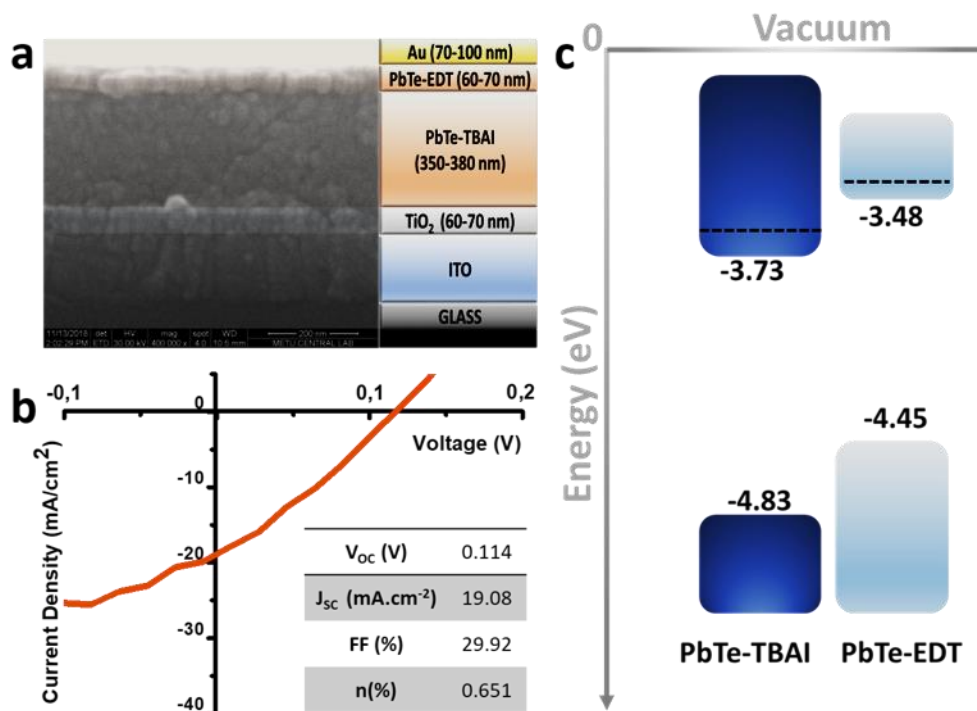


Figure 5. Solar cell characteristics of TBAI treated PbTe QDs. a) SEM image of a cell cross-section with a device architecture of ITO/ TiO₂/ PbTe-TBAI/ PbTe-EDT/ Au. b) Current-voltage characteristics of the cell shown in a. c) Energy landscape of the cell.

In light of the energy landscape determined from UPS measurements, we fabricated solar cells where TBAI treated PbTe QDs, with 1.26 eV band gap (in solution) and size in the range of 4-5 nm (see Figure 1c), were utilized as the light absorbing layer. A thin layer of EDT treated PbTe QDs was spin coated on TBAI treated layer to optimize the band alignment in the cell. In accordance with the UPS studies and previous reports, EDT treated layer is expected to act as a hole transport and exciton blocking layer [13]. SEM image of the solar cell cross-section is displayed in Figure 5a. TiO₂ with a thickness of 60-70 nm and Au (70-100 nm) were used as electron transport layer and cathode, respectively. The thicknesses of the TBAI and EDT treated layers were measured as 350-380 nm and 60-70 nm, respectively. The current voltage characteristic of the cell, measured with an ASTM Class A solar simulator with AM1.5G sun irradiance (100 mW/cm²), is presented in Figure 5b. The short circuit current density was measured as 19.08 mA.cm⁻² from a cell with an active area of 4.5 mm². The cell exhibited an open circuit voltage of 0.114 V and PCE of 0.651%. Although band alignment engineering leads to working solar cells based on PbTe QDs, solar cell efficiencies lag behind the other members of the lead chalcogenide family (PbS and PbSe QDs). Limited cell efficiencies of the solar cells fabricated in this study can be ascribed mainly to the presence of mid gap states which have adverse effects on open circuit voltage values. Future studies aiming to improve the material quality by optimizing surface passivation methods might reduce the open circuit voltage deficit and lead to record efficiencies in near future.

4. Conclusion and Comment

In conclusion, we fabricated solution based solar cells based on highly crystalline PbTe QDs and reached promising cell efficiencies. Control over TOP-Te injection/growth temperature allowed us to tune the size and band gap of the QDs. XRD and TEM results showed that QDs have high crystallinity and exhibit a preferential growth along {200} direction. Strong dependence of the band levels on the ligand type was discovered by UPS studies. Conduction and valence band levels of TBAI and EDT treated layers with respect to vacuum were determined as -3.73 eV/-4.83 eV and -3.48 eV/-4.45 eV, respectively. Band bending, attributed to the conduction band offset of 0.25 eV and valence band offset of 0.38 eV, between TBAI and EDT treated layers allowed us to fabricate solar cell with a bilayer architecture. We believe that further optimization of the electron collecting TiO₂ layer by doping, or replacement of TiO₂ with ZnO, which has better band alignment with the valence/conduction bands of QDs, will lead to further enhancement of the cell parameters in near future.

Author Statement

All the authors are responsible for the entire content of the study.

Acknowledgment

Solar cell fabrication and characterization processes were carried out at Atılım University, ATOMSEL under supervision of Prof. Dr. Atilla Cihaner. XPS/UPS, SEM and TEM measurements were performed at METU Central Laboratory. This work was supported by the The Scientific and Technological Research Council of Turkey (TÜBİTAK); Project Number 115F187 and Project Number: 117E787.

Conflict of Interest

As the authors of this study, we declare that we do not have any support and thank you statement.

Ethics Committee Approval and Informed Consent

As the authors of this study, we declare that we do not have any ethics committee approval and/or informed consent statement.

References

- [1] E. M. Sanehira, A. R. Marshall, J. A. Christians, S. P. Harvey, P. N. Ciesielski, L. M. Wheeler, P. Schulz, L. Y. Lin, M. C. Beard, and J. M. Luther, "Enhanced mobility CsPbI₃ quantum dot arrays for record-efficiency, high-voltage photovoltaic cells," *Sci. Adv.*, 3, eaao4204, 2017.
- [2] Y. Shirasaki, G. J. Supran, M. G. Bawendi, and V. Bulović, "Emergence of colloidal quantum-dot light-emitting technologies," *Nat. Photonics*, 7, 933–933, 2013.
- [3] B. S. Mashford, M. Stevenson, Z. Popovic, C. Hamilton, Z. Q. Zhou, C. Breen, J. Steckel, V. Bulovic, M. Bawendi, S. Coe-Sullivan, and P. T. Kazlas, "High-efficiency quantum-dot light-emitting devices with enhanced charge injection," *Nat. Photonics*, 7, 407–412, 2013.
- [4] J. Xu, O. Voznyy, M. Liu, A. R. Kirmani, G. Walters, R. Munir, M. Abdelsamie, A. H. Proppe, A. Sarkar, F. P. García de Arquer, M. Wei, B. Sun, M. Liu, O. Ouellette, R. Quintero-Bermudez, J. Li, J. Fan, L. Quan, P. Todorovic, H. Tan, S. Hoogland, S. O. Kelley, M. Stefiik, A. Amassian, and E. H. Sargent, "2D matrix engineering for homogeneous quantum dot coupling in photovoltaic solids," *Nat. Nanotechnol.*, 13, 456–462, 2018.
- [5] G. Konstantatos, I. Howard, A. Fischer, S. Hoogland, J. Clifford, E. Klem, L. Levina, and E. H. Sargent, "Ultrasensitive solution-cast quantum dot photodetectors," *Nature*, 442, 180–183, 2006.
- [6] A. H. Ip, S. M. Thon, S. Hoogland, O. Voznyy, D. Zhitomirsky, R. Debnath, L. Levina, L. R. Rollny, G. H. Carey, A. Fischer, K. W. Kemp, I. J. Kramer, Z. J. Ning, A. J. Labelle, K. W. Chou, A. Amassian, and E. H. Sargent, "Hybrid passivated colloidal quantum dot solids," *Nat. Nanotechnol.*, 7, 577–582, 2012.
- [7] D. Asil, B. J. Walker, B. Ehrler, Y. Vaynzof, A. Sepe, S. Bayliss, A. Sadhanala, P. C. Y. Chow, P. E. Hopkinson, U. Steiner, N. C. Greenham, and R. H. Friend, "Role of PbSe structural stabilization in photovoltaic cells," *Adv. Funct. Mater.*, 25, 928–935, 2015.
- [8] T. Haciefendioğlu, T. K. Solmaz, M. Erkan, and D. Asil, "A comprehensive approach for the instability of PbTe quantum dots and design of a combinatorial passivation strategy," *Sol. Energy Mater. Sol. Cells*, 207, 110362, 2020.
- [9] M. L. Böhm, T. C. Jellicoe, M. Tabachnyk, N. J. L. K. Davis, F. Wisnivesky-Rocca-Rivarola, C. Ducati, B. Ehrler, A. A. Bakulin, and N. C. Greenham, "Lead telluride quantum dot solar cells displaying external quantum efficiencies exceeding 120%," *Nano Lett.*, 15, 7987–7993, 2015.
- [10] W. K. Bae, J. Joo, L. A. Padilha, J. Won, D. C. Lee, Q. Lin, W. Koh, H. Luo, V. I. Klimov, and J. M. Pietryga, "Highly effective surface passivation of pbse quantum dots through reaction with molecular chlorine," *J. Am. Chem. Soc.*, 134, 20160–20168, 2012.
- [11] Q. Lin, H. J. Yun, W. Liu, H.-J. Song, N. S. Makarov, O. Isaienko, T. Nakotte, G. Chen, H. Luo, V. I. Klimov, and J. M. Pietryga, "Phase-transfer ligand exchange of lead chalcogenide quantum dots for direct deposition of thick, highly conductive films," *J. Am. Chem. Soc.*, 139, 6644–6653, 2017.
- [12] H. Zhang, J. Jang, W. Liu, and D. V. Talapin, "Colloidal nanocrystals with inorganic halide, pseudohalide, and halometallate ligands," *ACS Nano*, 8, 7359–7369, 2014.
- [13] C.-H. M. Chuang, P. R. Brown, V. Bulović, and M. G. Bawendi, "Improved performance and stability in quantum dot solar cells through band alignment engineering," *Nat. Mater.*, 13, 796–801, 2014.
- [14] J. J. Urban, D. V. Talapin, E. V. Shevchenko, and C. B. Murray, "Self-Assembly of PbTe quantum dots into nanocrystal superlattices and glassy films," *J. Am. Chem. Soc.*, 128, 3248–3255, 2006.
- [15] J. E. Murphy, M. C. Beard, A. G. Norman, S. P. Ahrenkiel, J. C. Johnson, P. Yu, O. I. Mičić, R. J. Ellingson, and A. J. Nozik, "PbTe colloidal nanocrystals: Synthesis, characterization, and multiple exciton generation," *J. Am. Chem. Soc.*, 128, 3241–3247, 2006.
- [16] W. Lu, J. Fang, K. L. Stokes, and J. Lin, "Shape Evolution and Self Assembly of Monodisperse

- PbTe Nanocrystals,” *J. Am. Chem. Soc.*, 126, 11798–11799, 2004.
- [17] L. Yang, M. Tabachnyk, S. L. Bayliss, M. L. Böhm, K. Broch, N. C. Greenham, R. H. Friend, and B. Ehrler, “Solution-Processable Singlet Fission Photovoltaic Devices,” *Nano Lett.*, 15, 354–358, 2015.
- [18] A. B. Mandale and S. Badrinarayanan, “X-ray photoelectron spectroscopic studies of the semimagnetic semiconductor system $\text{Pb}_{1-x}\text{Mn}_x\text{Te}$,” *J. Electron Spectros. Relat. Phenomena.*, 53 (1-2), 87–95, 1990.
- [19] E. A. Kraut, R. W. Grant, J. R. Waldrop, and S. P. Kowalczyk, “Semiconductor core-level to valence-band maximum binding-energy differences: Precise determination by x-ray photoelectron spectroscopy,” *Phys. Rev. B*, 28, 1965–1977, 1983.